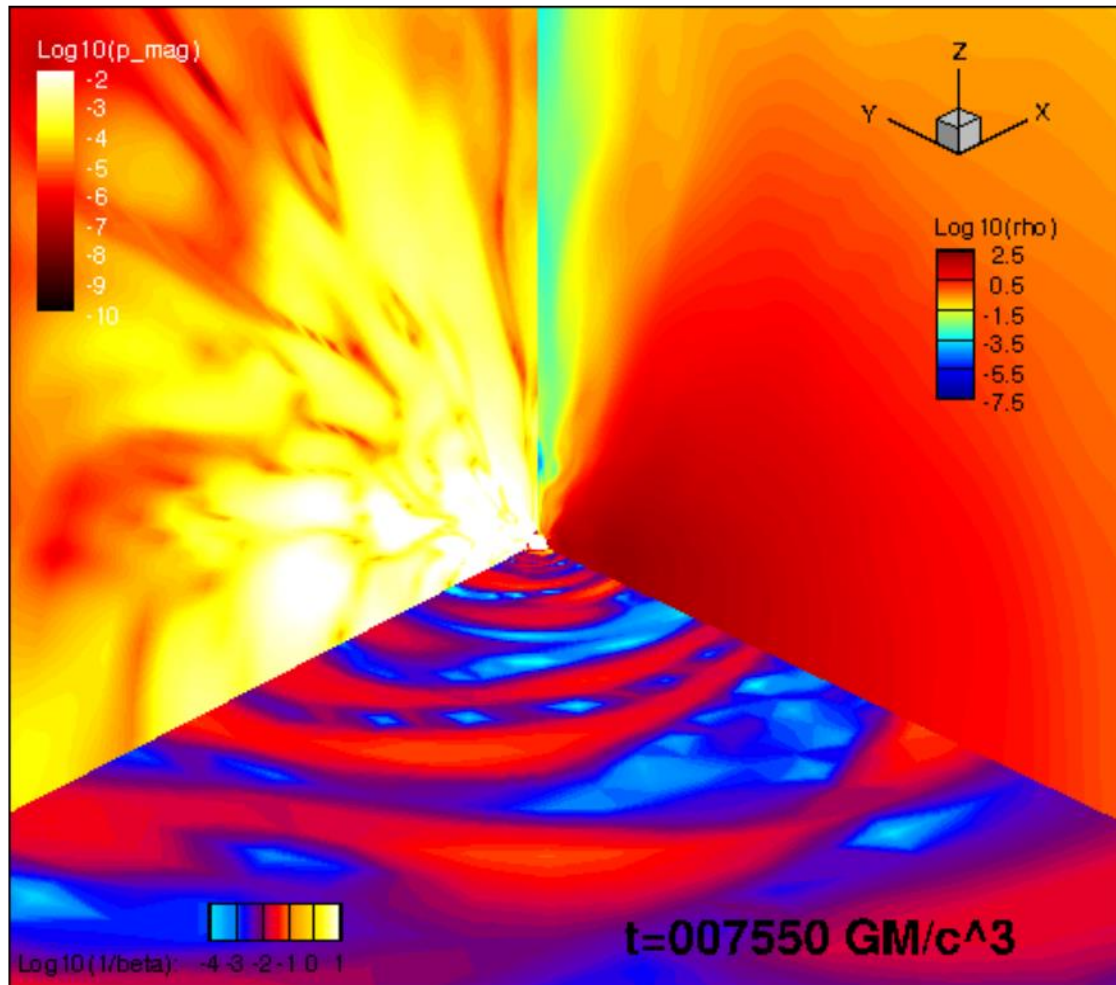


# 大質量ブラックホール降着円盤から放出される 大強度アルファヴェンパルスとジェット



水田 晃(理化学研究所)

References

AM, Ebisuzaki Tajima Nagataki,  
MNRAS 479 2534(2018)

the case of spin  $a=0.9$

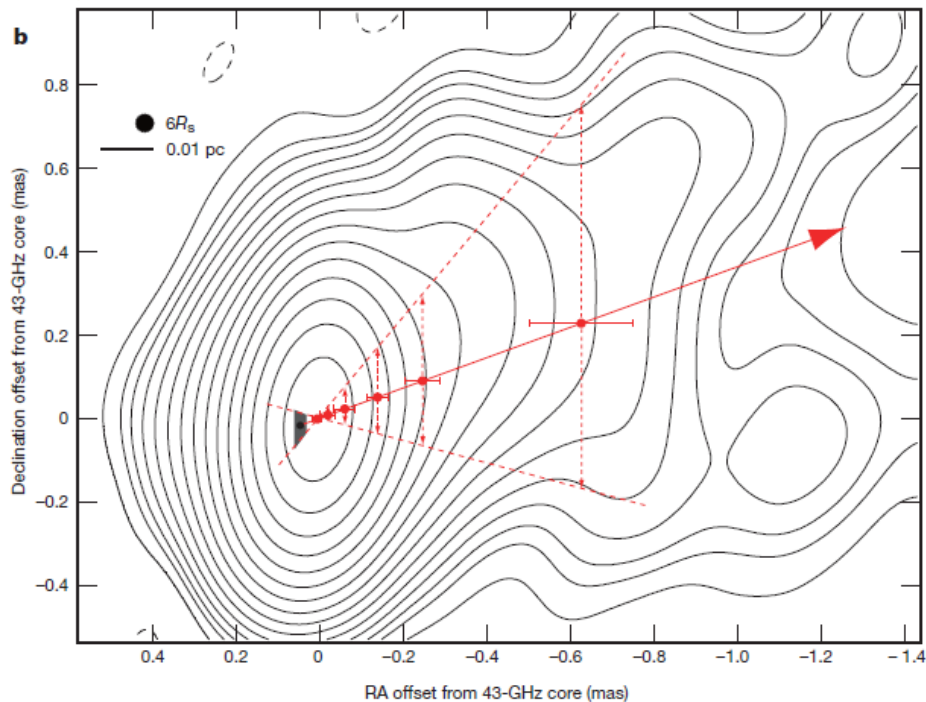
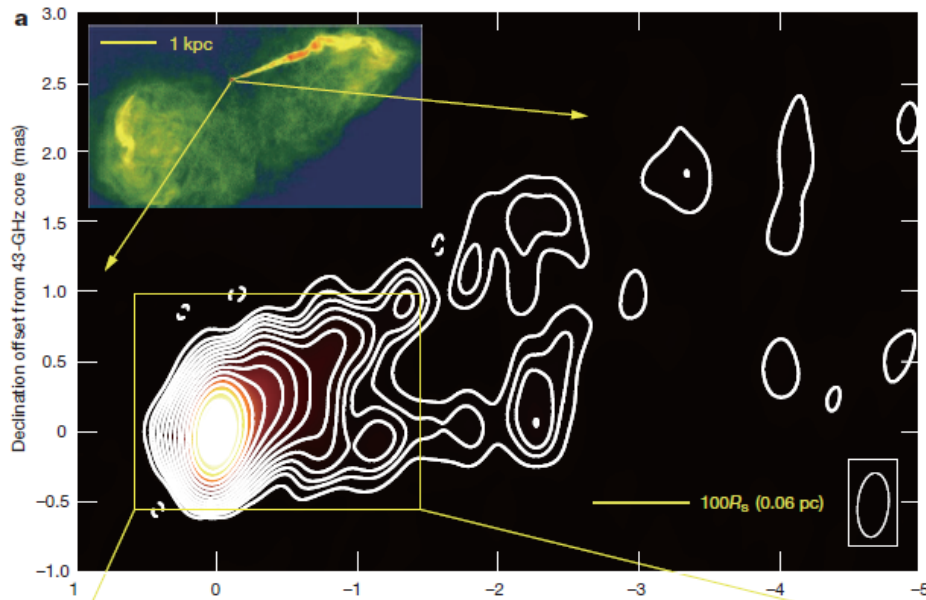
AM+ in prep.

parameter study in spin  $a$

高エネルギー天体現象の多様性

@東大宇宙線研 18.11.20-21

# Active Galactic Nuclei Jet



Highly collimated outflows from center of galaxy

- central engine  
supermassive black hole

+

accretion disk

- relativistic outflows

Bulk Lorentz factor :  $\Gamma \sim 10$

- multiwavelength emission  
radio to high energy  $\gamma$ -rays

- strong candidate of  
ultra high energy cosmic ray  
accelerator

via Fermi acc. ? (1954)

wake field acc.

(Ebisuzaki & Tajima 2014)

M87 radio observation Hada +(2011)

# ブラックホール降着円盤とジェット形成

中心エンジン (Black Hole(BH) + disk)

-円盤の時間変動 (Shibata +1990,  
Balbus & Hawley1991)

-- MRI growth ( $B \nearrow \Rightarrow$  Low beta state)

Magnetorotational instability(磁気回転不安定性)

- 差動回転:  $d\Omega_{\text{disk}}/dr < 0$

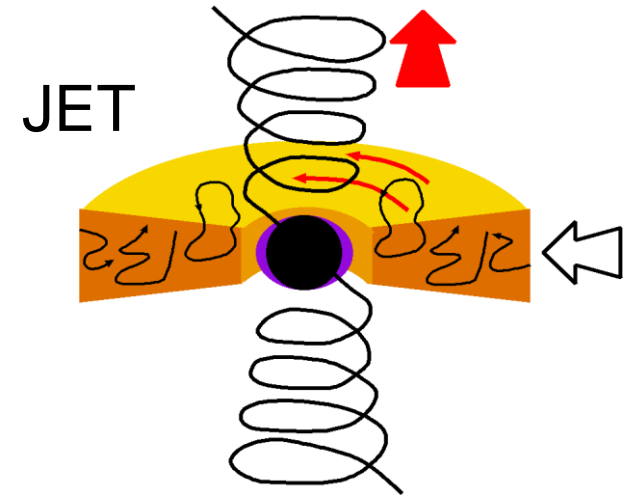
$\Omega_{\text{disk}} \propto r^{-1.5}$  :Kepler rotation

-  $B \propto \exp(i\omega t)$  指数関数的増幅

Unstable @  $0 < kV_a < 1.73 \Omega_K$

Most unstable @  $kV_a \sim \Omega_K$   $\omega \sim 0.75\Omega_K$

- MRI によって角運動量輸送



-- 磁気エネルギーの散逸 ( $B \searrow \Rightarrow$  High beta state)

-- 円盤鉛直方向に Strong Alfvén burst (Low  $\beta \Rightarrow$  High  $\beta$ )

ジェット中を伝播し、wake field 加速機構による宇宙線の起源や  
ブレイザー天体の短時間変動 (Ebisuzaki +2014, A.M2018)

# B-field amplification in the disk

## Magnetorotational instability (MRI)

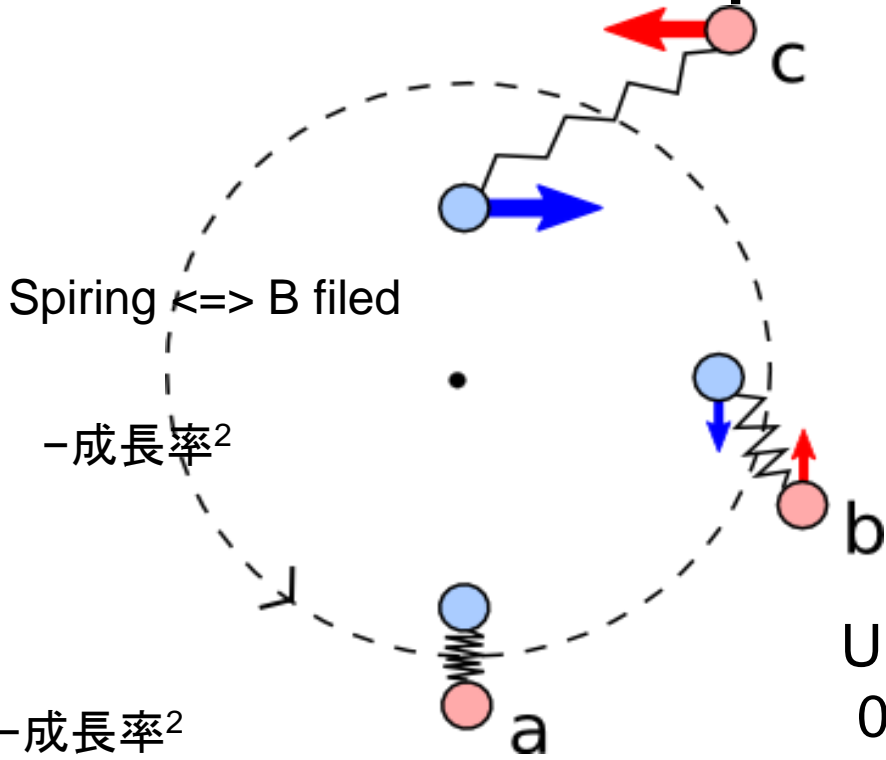
– differentially rotating disk :

$$d\Omega_{\text{disk}}/dr < 0$$

$$\Omega_{\text{disk}} \propto r^{-1.5} \quad \text{: Kepler rotation}$$

–  $B \propto \exp(i\omega t)$

– MRI enhances angular momentum transfer



Unstable @

$$0 < kV_a < 1.73 \Omega_K$$

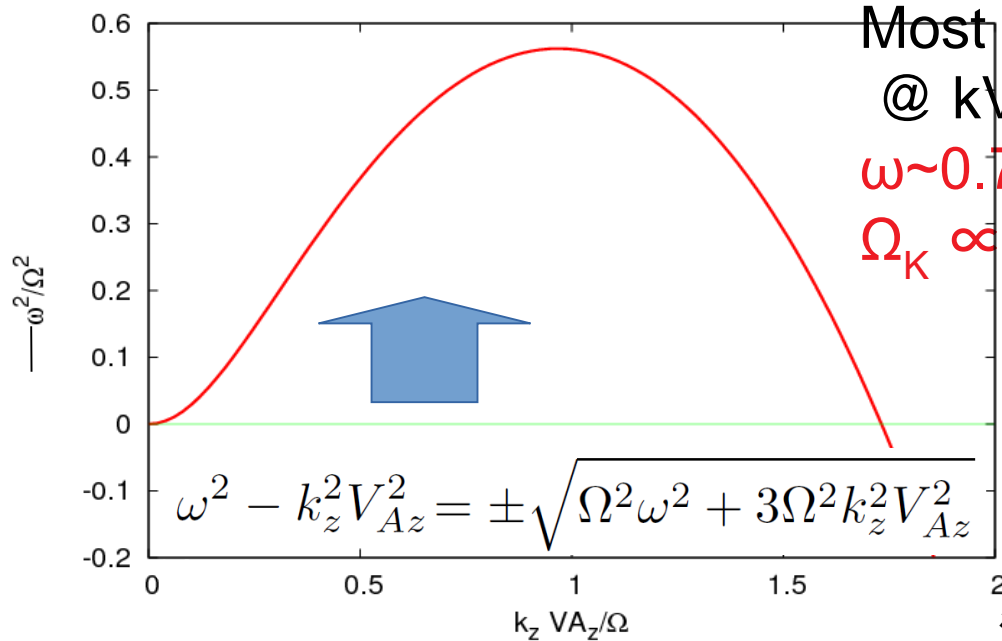
Most unstable

$$@ kV_a \sim \Omega_K$$

$$\omega \sim 0.75 \Omega_K$$

$$\Omega_K \propto R^{-3/2},$$

-成長率<sup>2</sup>



Velikhov (1959)

Chandrasekhar (1960)

Balbus & Hawley (1991)

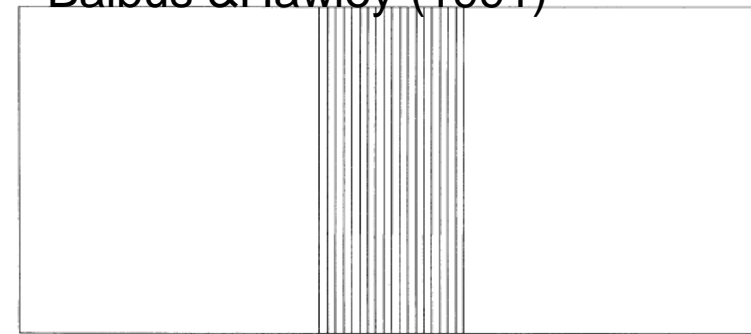


FIG. 3a

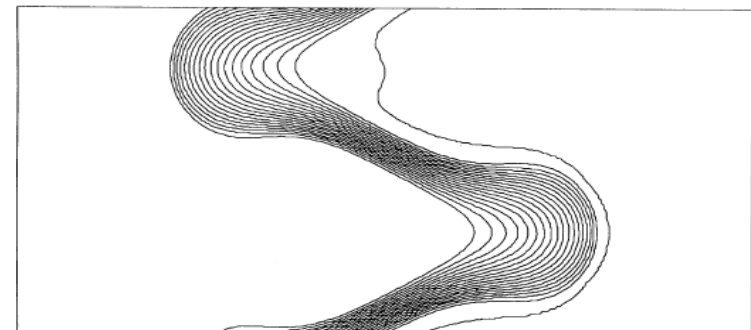


FIG. 3b

# Basic Equations : GRMHD Eqs.

$GM=c=1$ ,  $a$ : dimensionless Kerr spin parameter

$$\frac{1}{\sqrt{-g}}\partial_\mu(\sqrt{-g}\rho u^\mu) = 0 \quad \text{Mass conservation Eq.}$$

$$\partial_\mu(\sqrt{-g}T^\mu_\nu) = \sqrt{-g}T^\kappa_\lambda \Gamma^\lambda_{\nu\kappa} \quad \text{Energy-momentum conservation Eq.}$$

$$\partial_t(\sqrt{-g}B^i) + \partial_j(\sqrt{-g}(b^i u^j - b^j u^i)) = 0 \quad \text{Induction Eq.}$$

$$p = (\gamma - 1)\rho\epsilon \quad \text{EOS } (\gamma=4/3)$$

---

## Constraint equations.

$$\frac{1}{\sqrt{-g}}\partial_i(\sqrt{-g}B^i) = 0 \quad \text{No-monopoles constraint}$$

$$u_\mu b^\mu = 0 \quad \text{Ideal MHD condition}$$

$$u_\mu u^\mu = -1 \quad \text{Normalization of 4-velocity}$$

---

## Energy-momentum tensor

$$T^{\mu\nu} = (\rho h + b^2)u^\mu u^\nu + (p_g + p_{\text{mag}})g^{\mu\nu} - b^\mu b^\nu$$

$$p_{\text{mag}} = b^\mu b_\mu / 2 = b^2 / 2$$

$$b^\mu \equiv \epsilon^{\mu\nu\kappa\lambda} u_\nu F_{\lambda\kappa} / 2 \quad B^i = F^{*it}$$

---

## GRMHD code (Nagataki 2009,2011)

Kerr-Schild metric (no singular at event horizon)

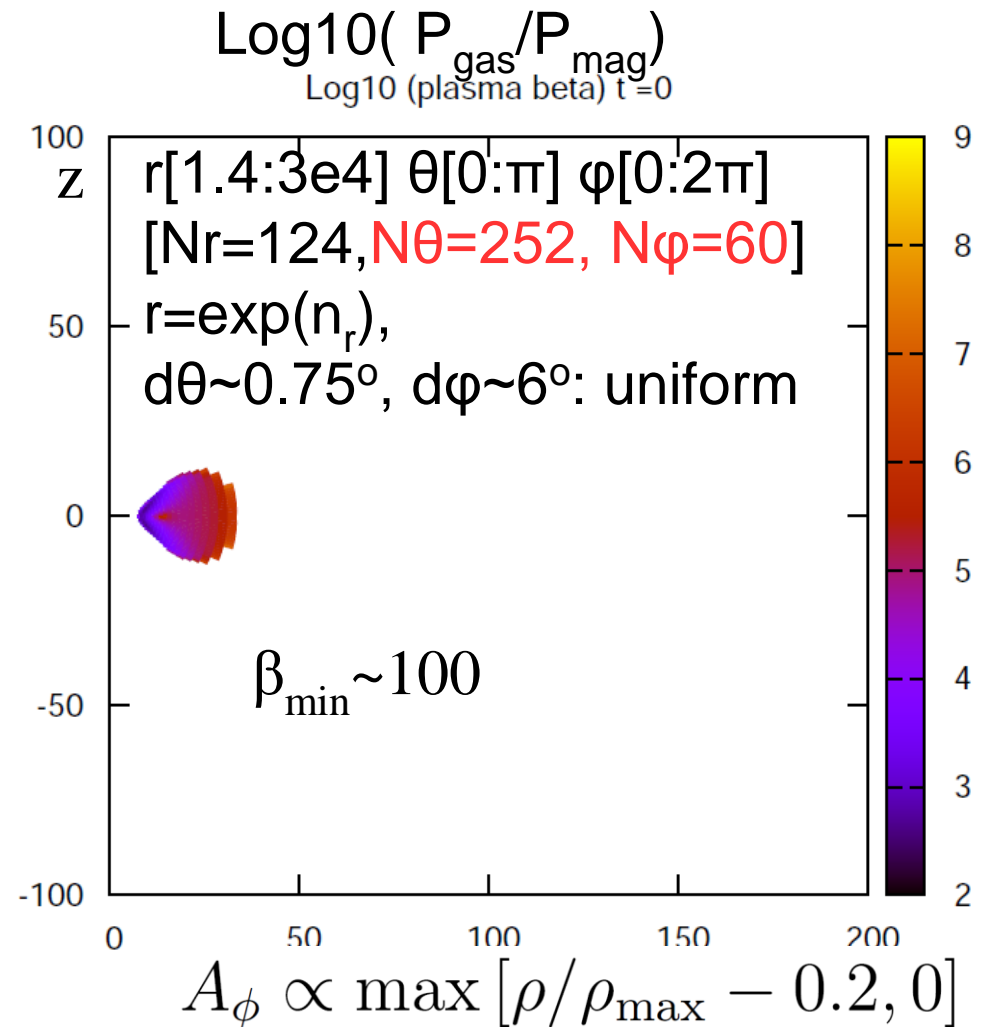
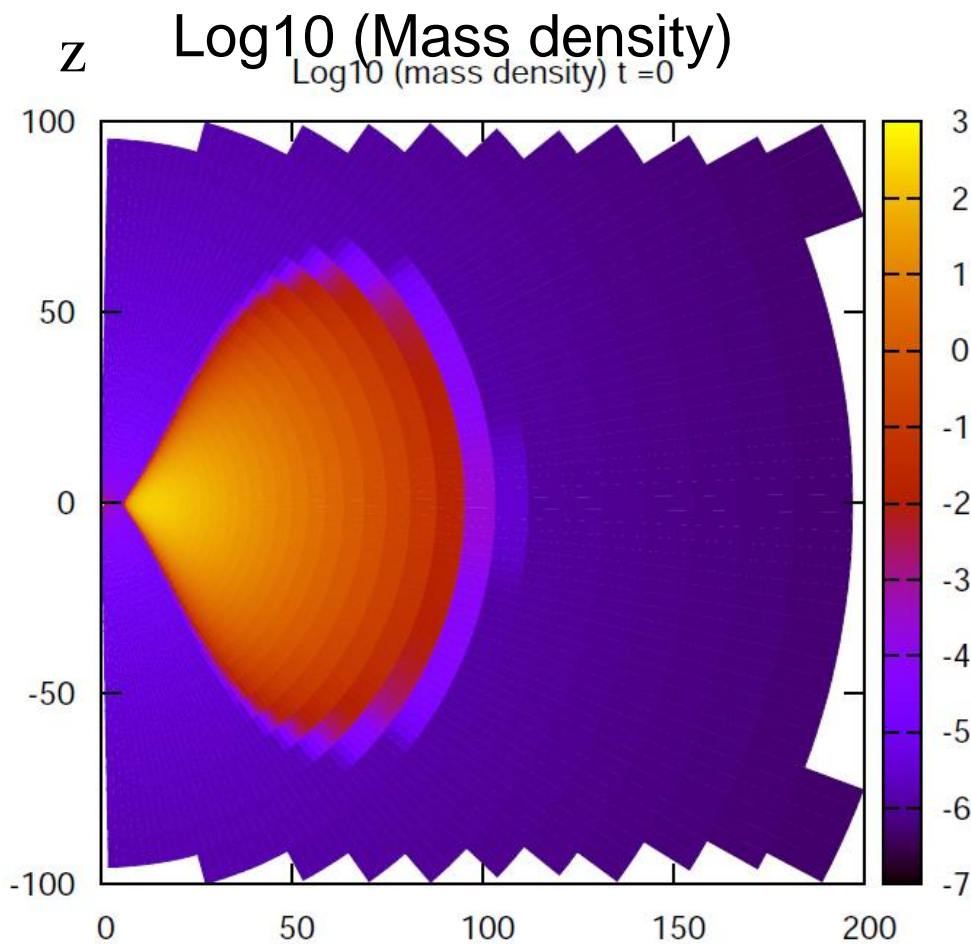
HLL flux, 2<sup>nd</sup> order in space (van Leer), 2<sup>nd</sup> or 3<sup>rd</sup> order in time

See also, Gammie +03, Noble + 2006

Flux-interpolated CT method for divergence free



# Initial Condition



Fisbone-Moncrief (1976) solution – hydrostatic solution of tori around rotating BH ( $a=0.9$ ,  $r_H \sim 1.44$ ),  $l_* \equiv -u^t u_\phi = \text{const} = 4.45$ ,  $r_{\text{in}} = 6. > r_{\text{ISCO}}$   
**With maximum 5% random perturbation in thermal pressure.**

**Units** L :  $R_g = GM/c^2$  (=Rs/2), T :  $R_g/c = GM/c^3$ , mass : scale free  
 $\sim 1.5 \times 10^{13} \text{cm} (M_{\text{BH}}/10^8 M_{\text{sun}})$   $\sim 500 \text{s} (M_{\text{BH}}/10^8 M_{\text{sun}})$

# Grids to capture MRI fastest growing mode

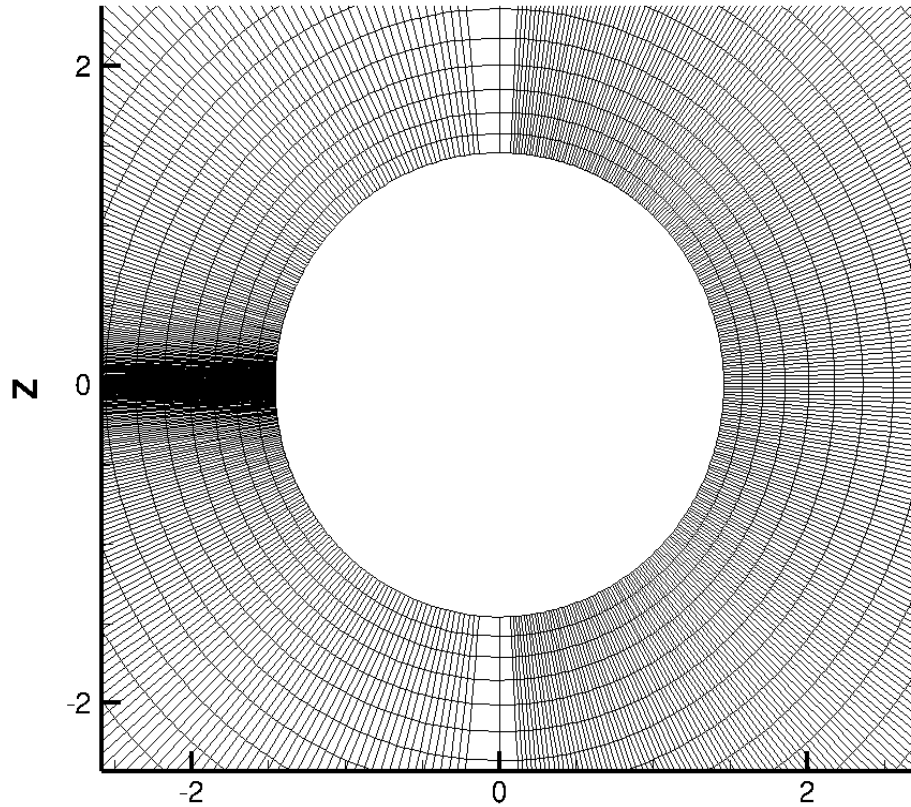
Wavelength of fastest growing mode in the disk

$$\lambda_{\text{MRI}} = 2\pi \langle C_{\text{az}} \rangle / \Omega_{\text{K}}(R) \sim 0.022 (R/R_{\text{ISCO}})^{1.5}$$

$$\langle C_s \rangle \sim \langle C_{\text{Az}} \rangle \sim 10^{-3} c$$

$$R_{\text{ISCO}}(a=0.9) = 2.32$$

$$N_{\theta} = 252$$



$$\theta = \pi x_2 + \frac{1}{2}(1-h) \sin(2\pi x_2) \quad \Delta\theta = \text{cost}$$

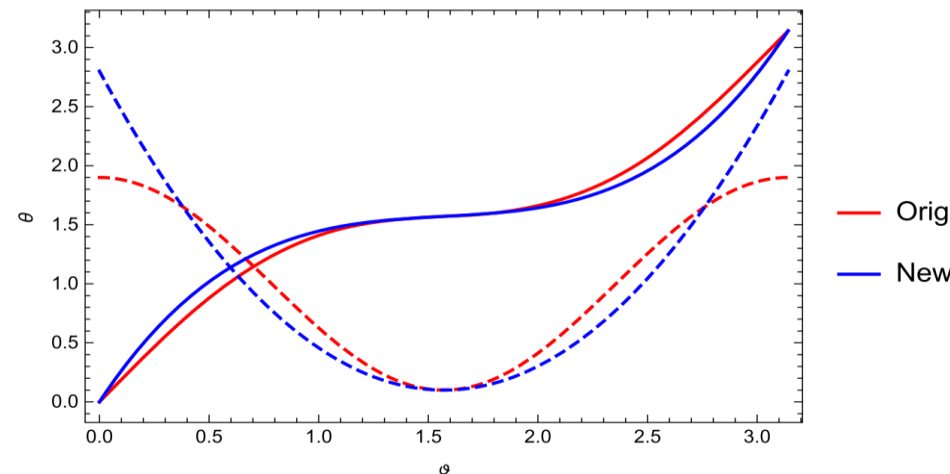
$$x_2 = [0:1] \quad \Delta x_2 = \text{cost} \quad h=1$$

$$h=0.2$$

McKinney and Gammie . . . .

Any coordinates described by analytic function can be applied (generalized curvilinear coordinates)

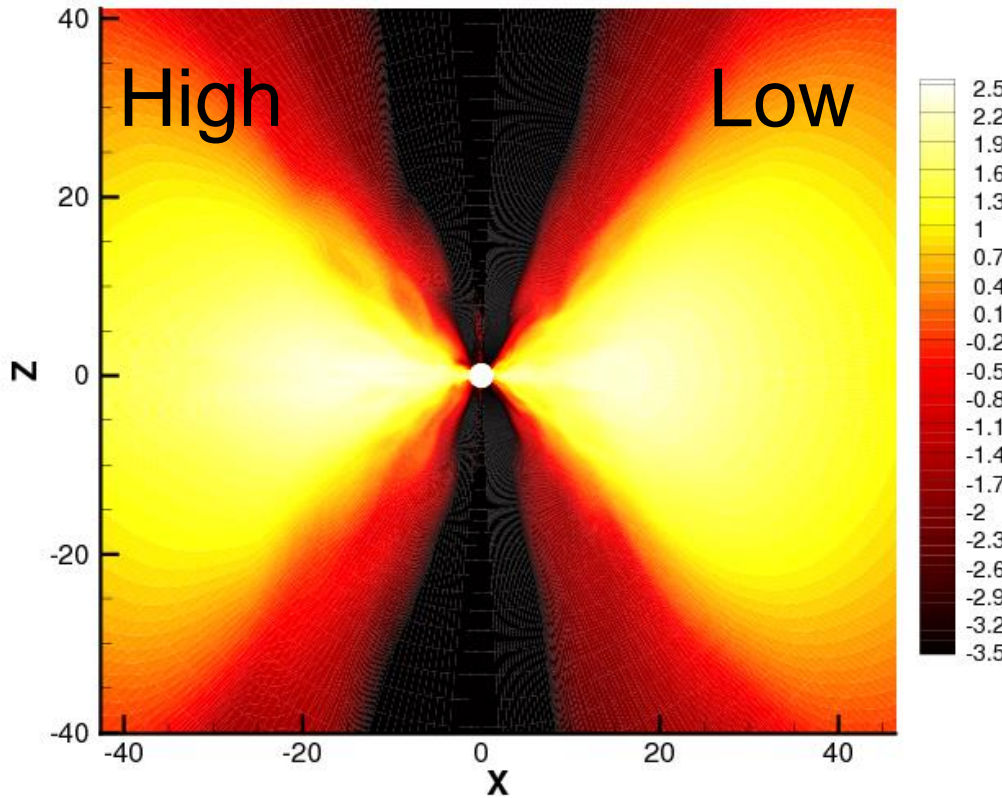
$$\theta_{\text{KS}}(\vartheta) = \vartheta + \frac{2h\vartheta}{\pi^2} (\pi - 2\vartheta)(\pi - \vartheta).$$



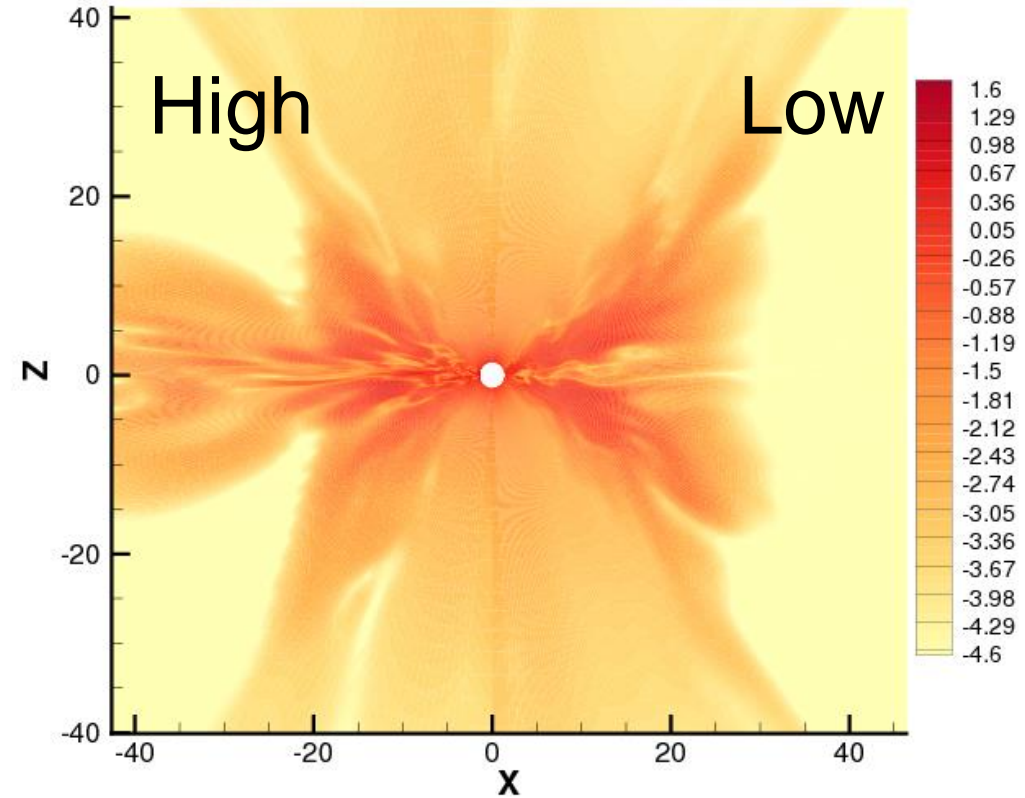
Porth + 2017

# Higher resolution calculation in $\theta$ around equator

Log10(Mass density)

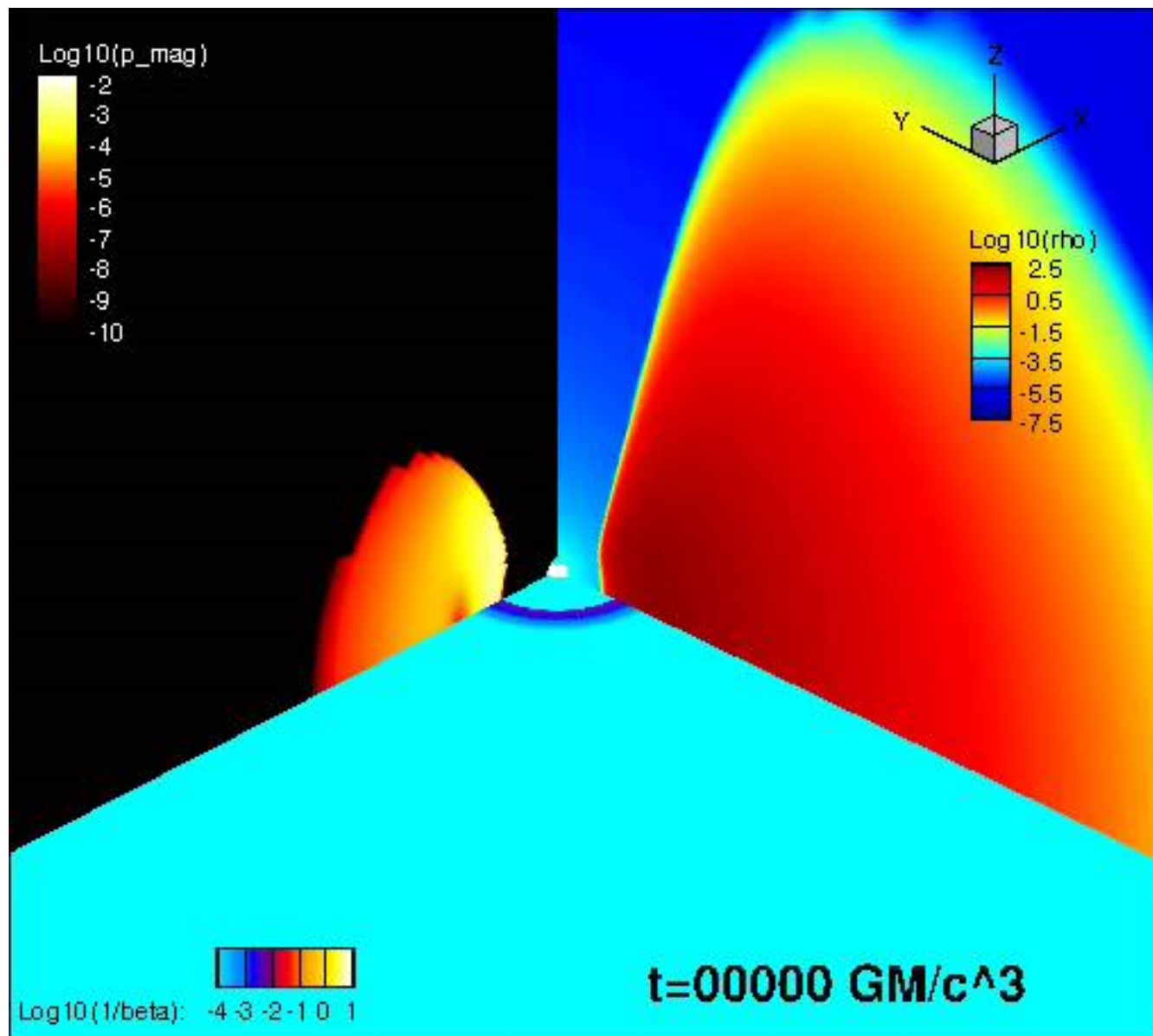


Log10(Magnetic pressure)



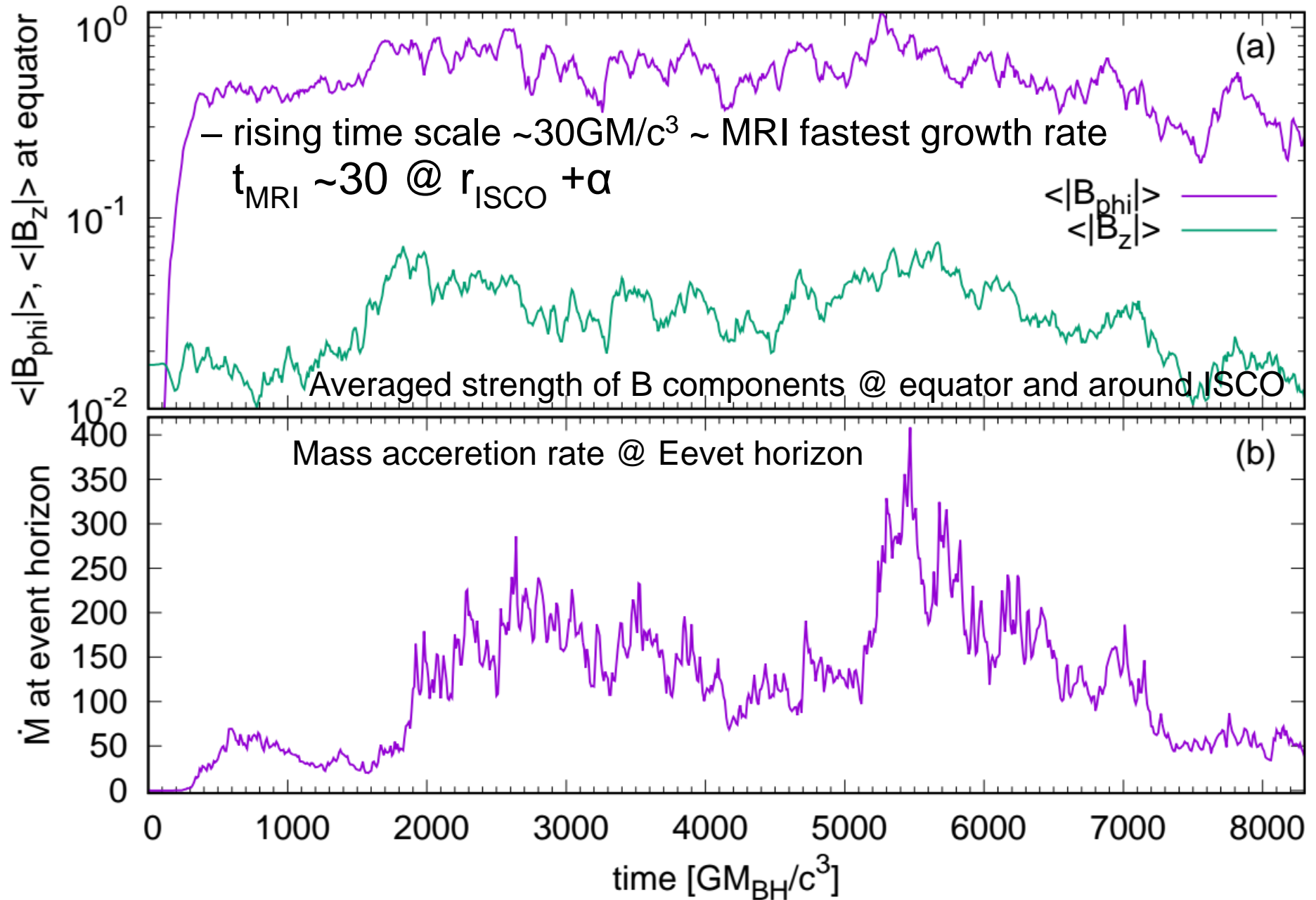
Right : about 8 times higher resolution in theta @ equator

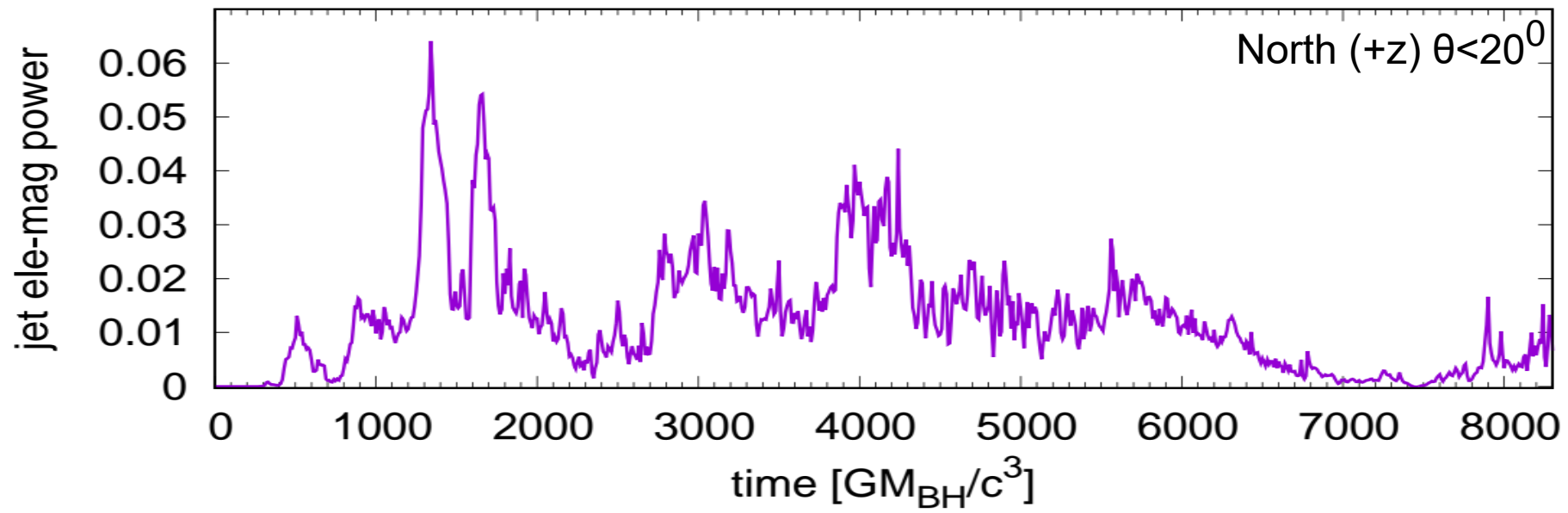


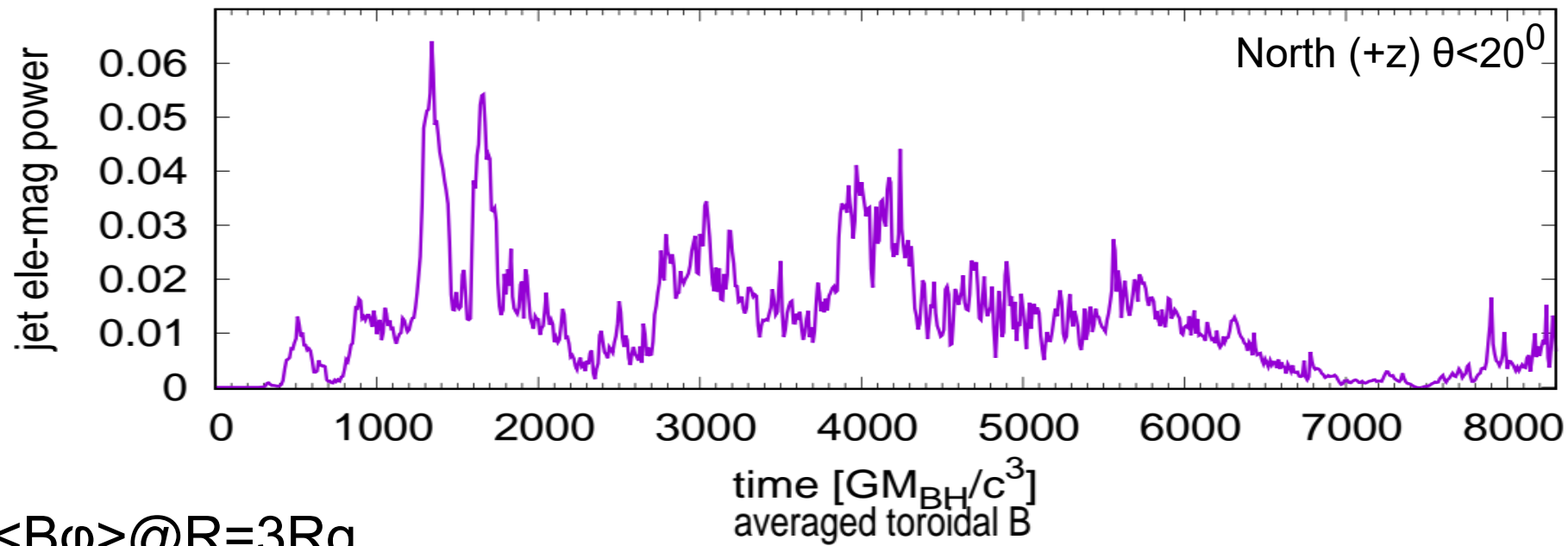


Disk : Fishbone Moncrief solution, spin parameter  **$a=0.9$  (0.7, 0.5, 0.3, 0.1)**  
 spherical coordinate  $R[0.98 r_H(a):3e4]$   $\theta[0:\pi]$   $\varphi[0:2\pi]$   
 $[NR=124, N\theta=252, N\varphi=60]$   $r=\exp(n_r)$ ,  $\theta$  : **non-uniform (concentrate @ equator)**  
 $d\varphi\sim 6^\circ$ : uniform Poloidal B field,  $\beta_{\min}=100$

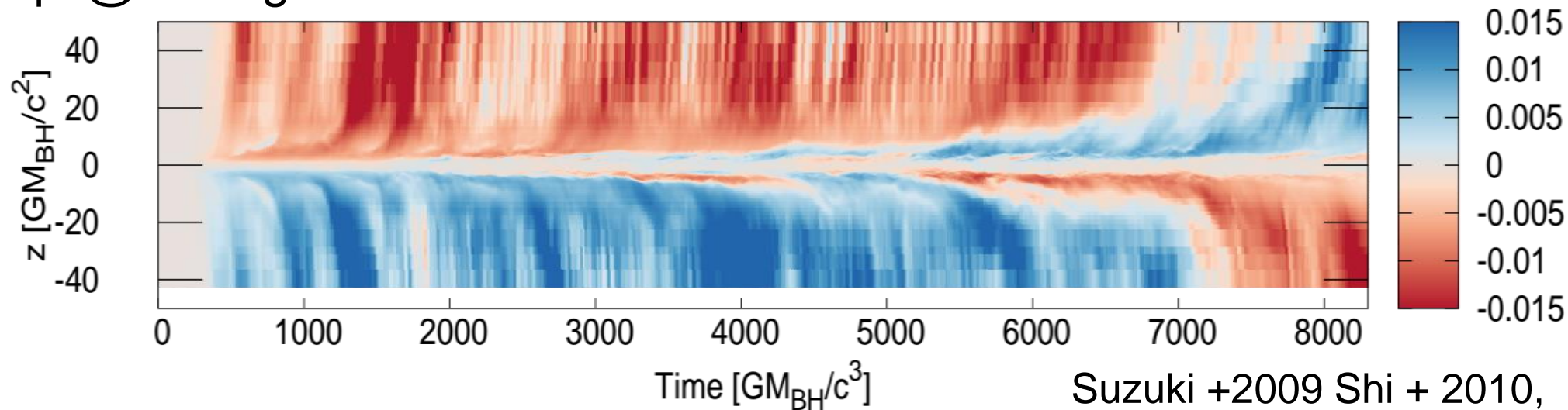
# B-field amplification & mass accretion





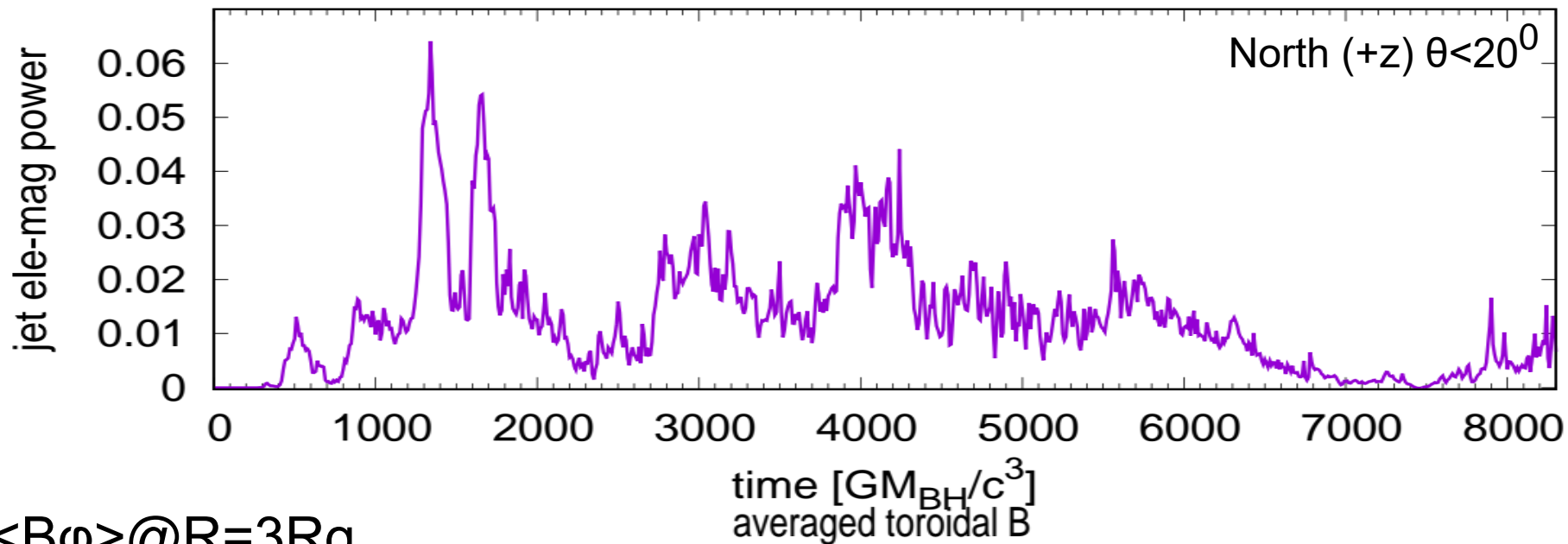


$\langle B_\phi \rangle @ R=3R_g$

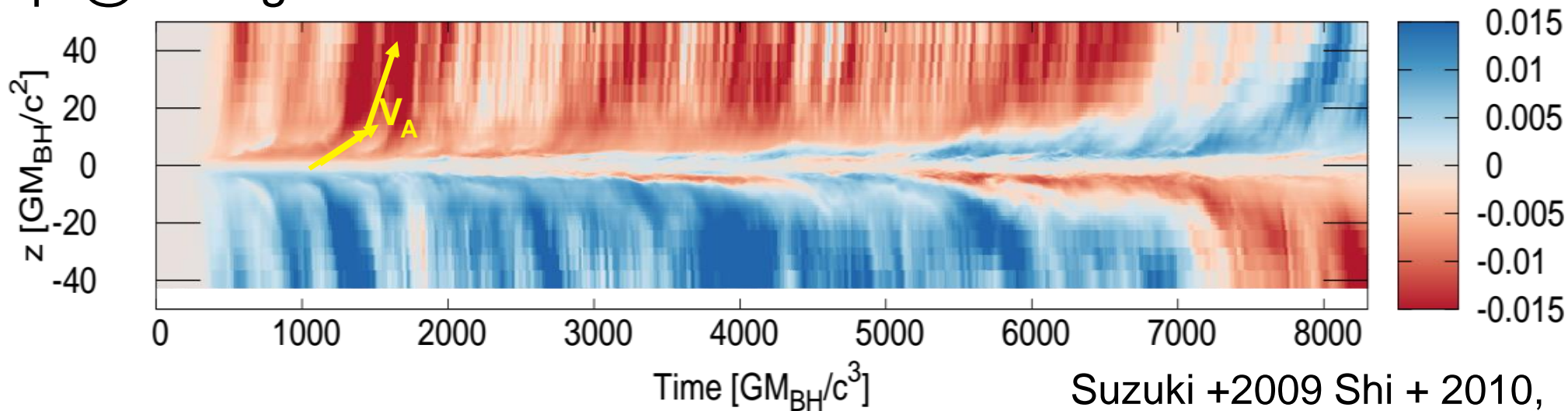


Suzuki +2009 Shi + 2010,  
Machida +2013

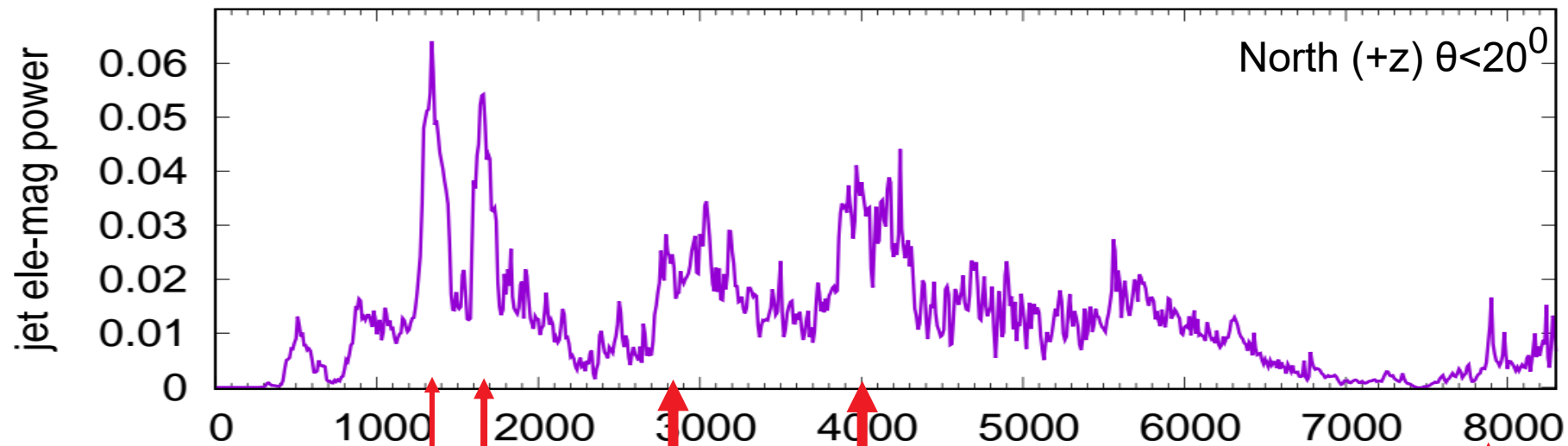




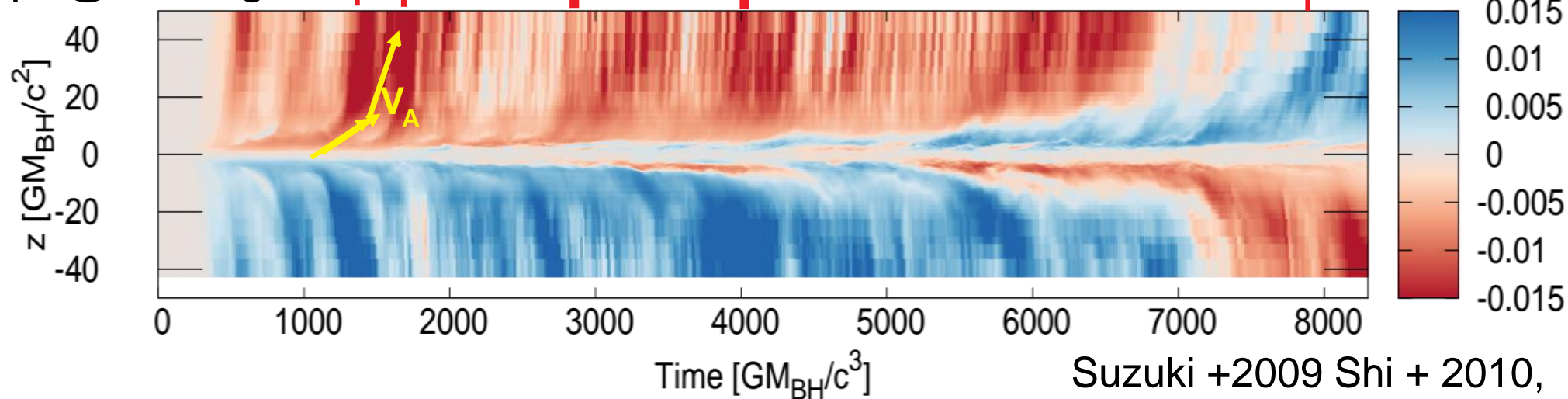
$\langle B_\phi \rangle @ R=3R_g$



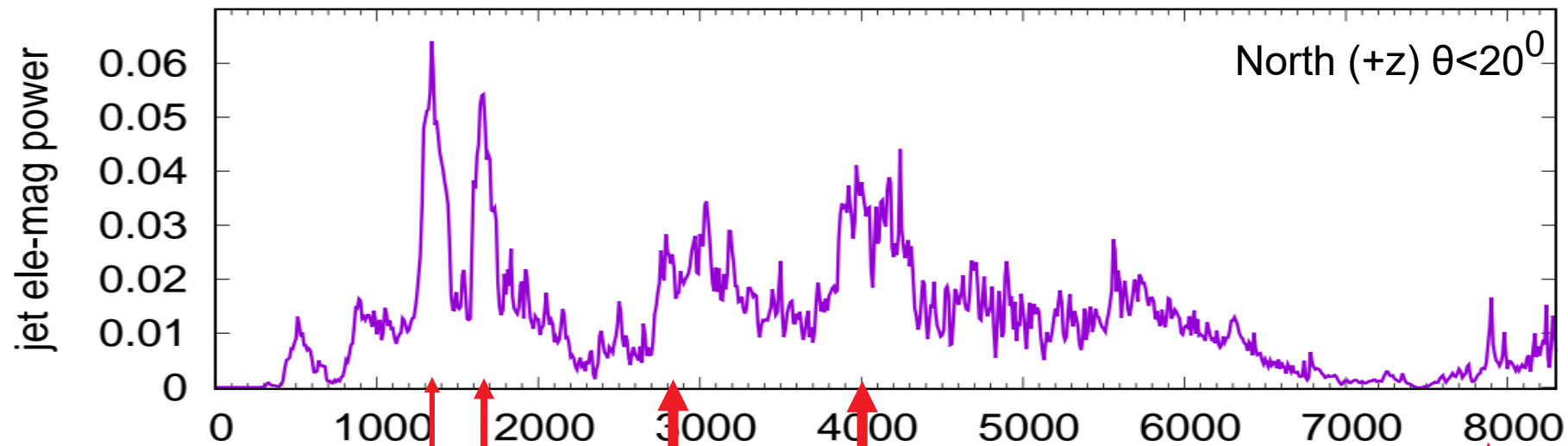
Suzuki +2009 Shi + 2010,  
Machida +2013



$\langle B_\phi \rangle @ R=3R_g$

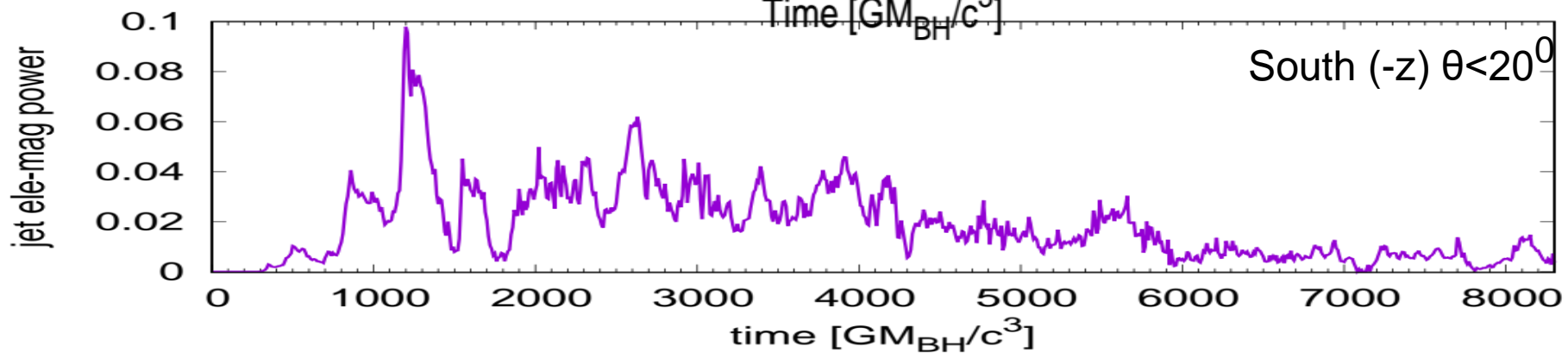
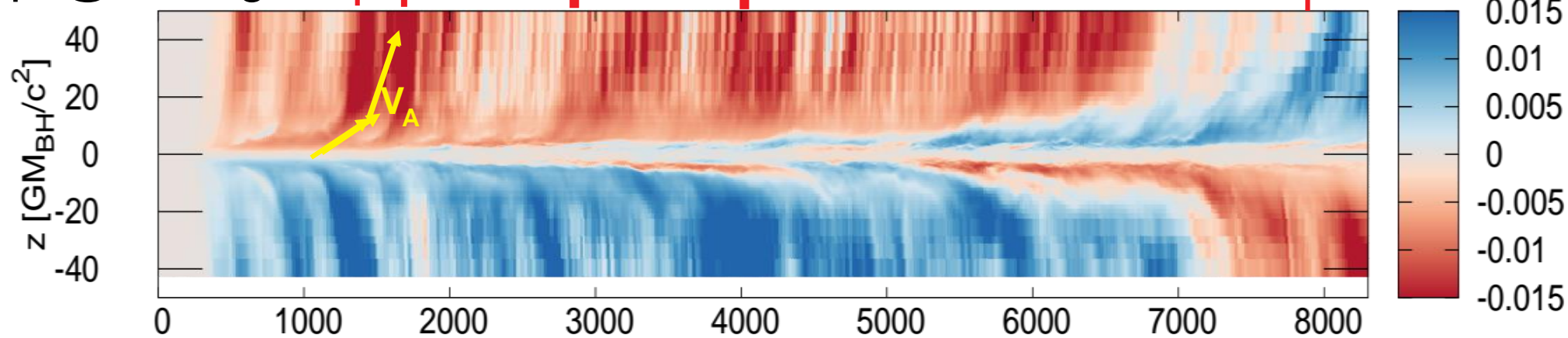


Suzuki +2009 Shi + 2010,  
Machida +2013  
Takasao+2018 =>後述



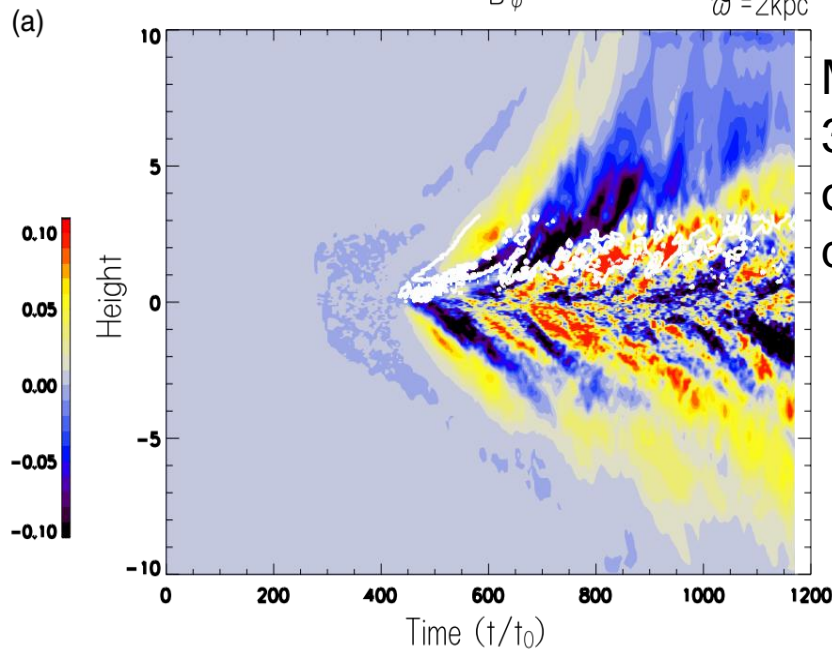
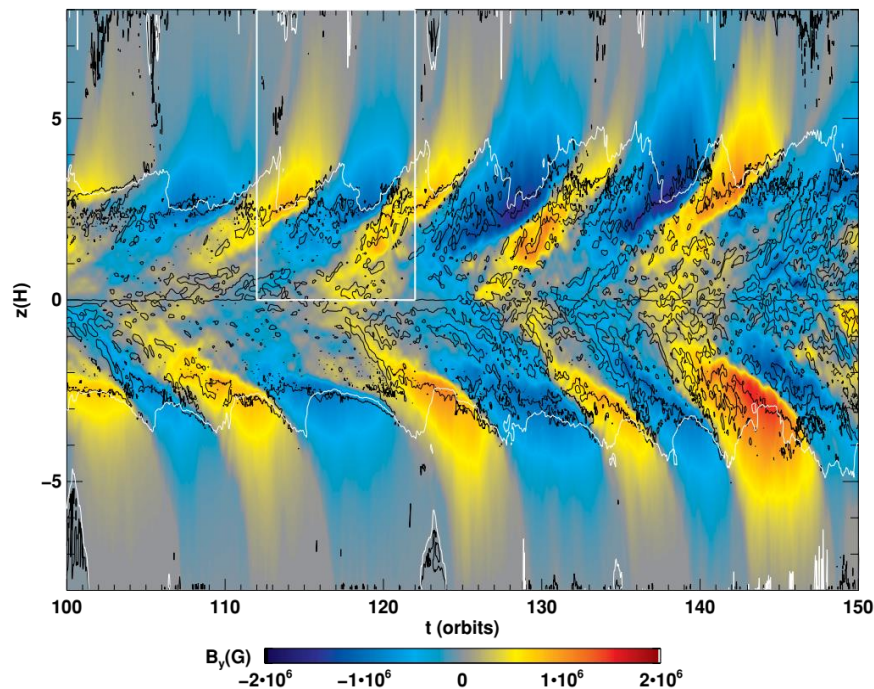
averaged toroidal B

$\langle B_\phi \rangle @ R=3R_g$





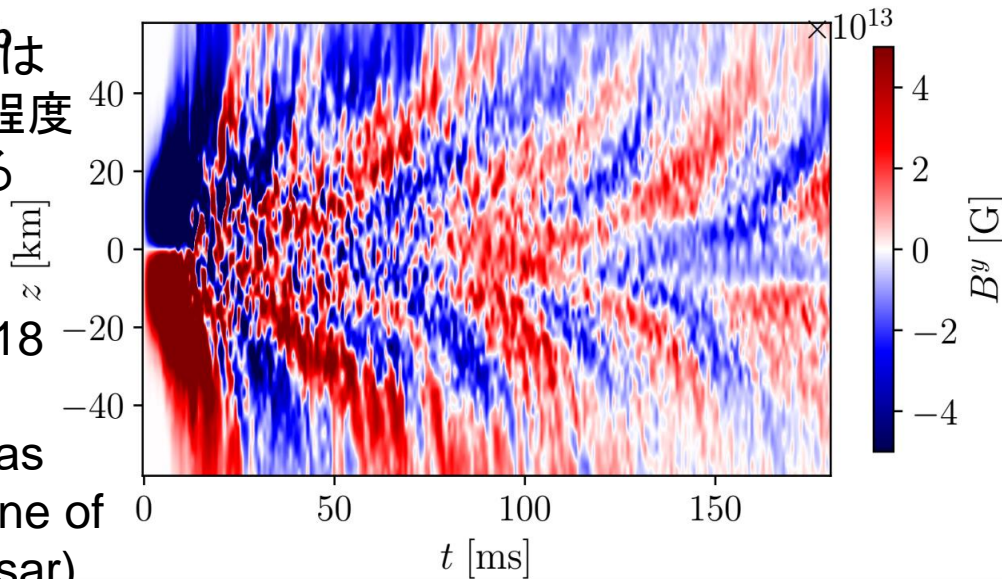
# Butterfly diagram is common feature of accretion disk



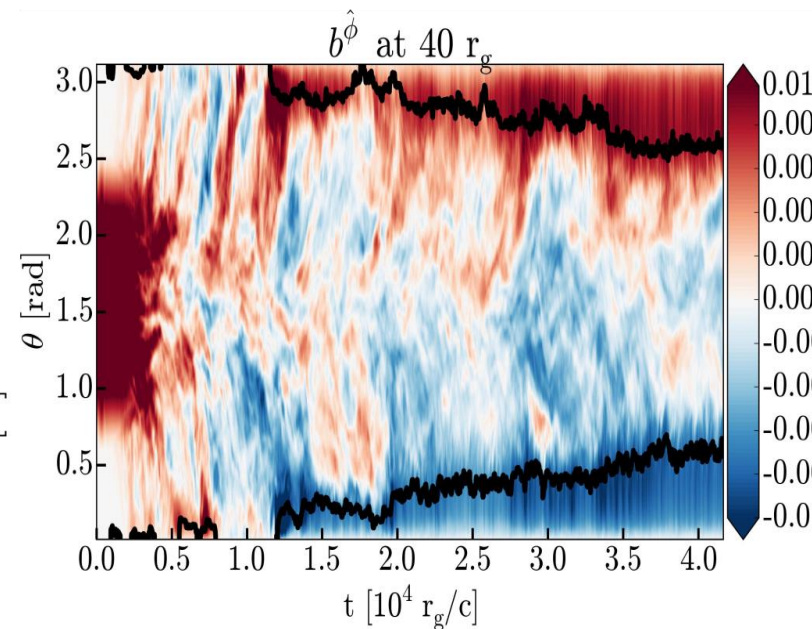
Machida + 2013  
3D MHD sim  
of galactic  
dynamo

Shi + 2011  
Local box sim.  
Protostellar disk

繰り返し周期は  
10回転周期程度  
極性が変わる



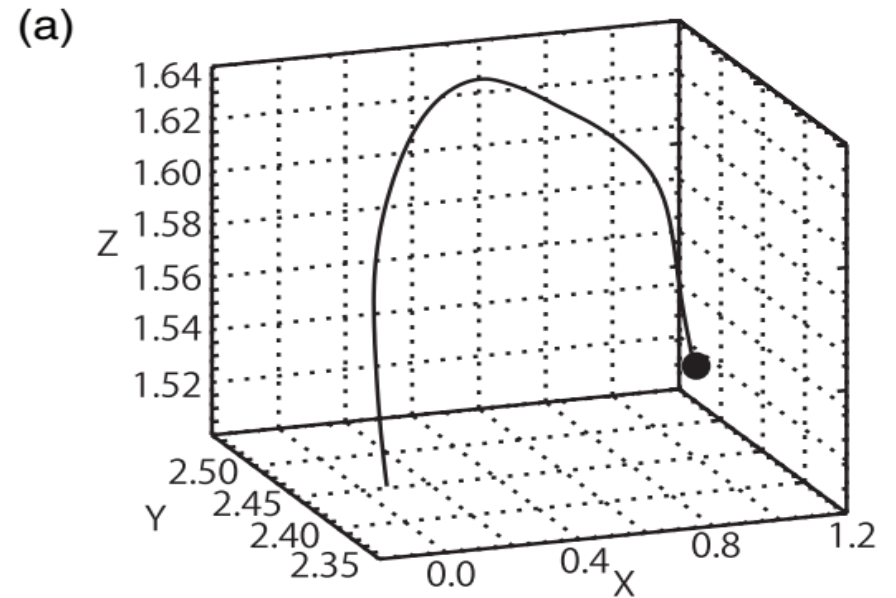
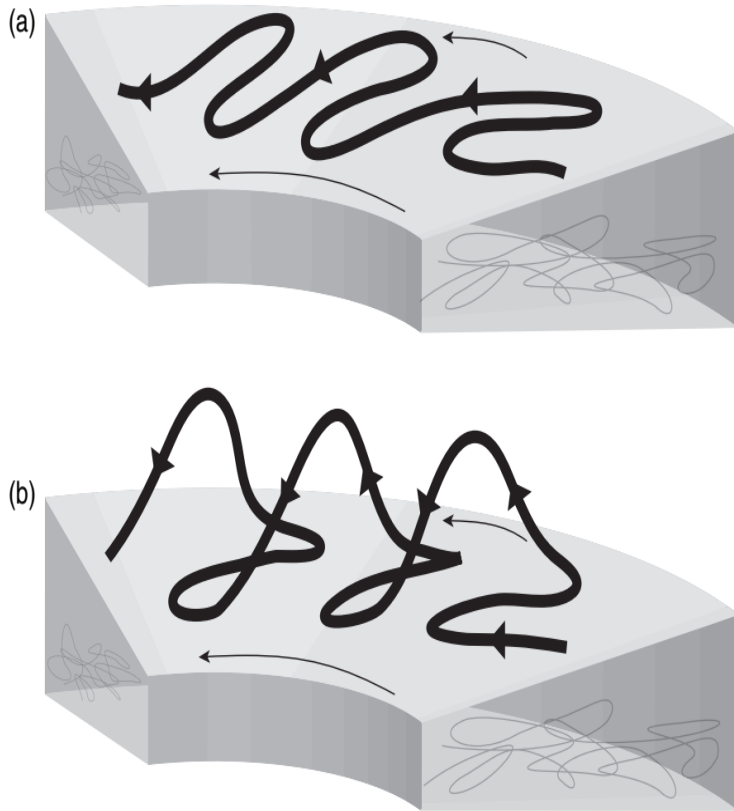
Siegel + 2018  
GRMHD  
+ v cooling as  
central engine of  
GRB(collapsar)



Liska + 2018  
GRMHD+AMR



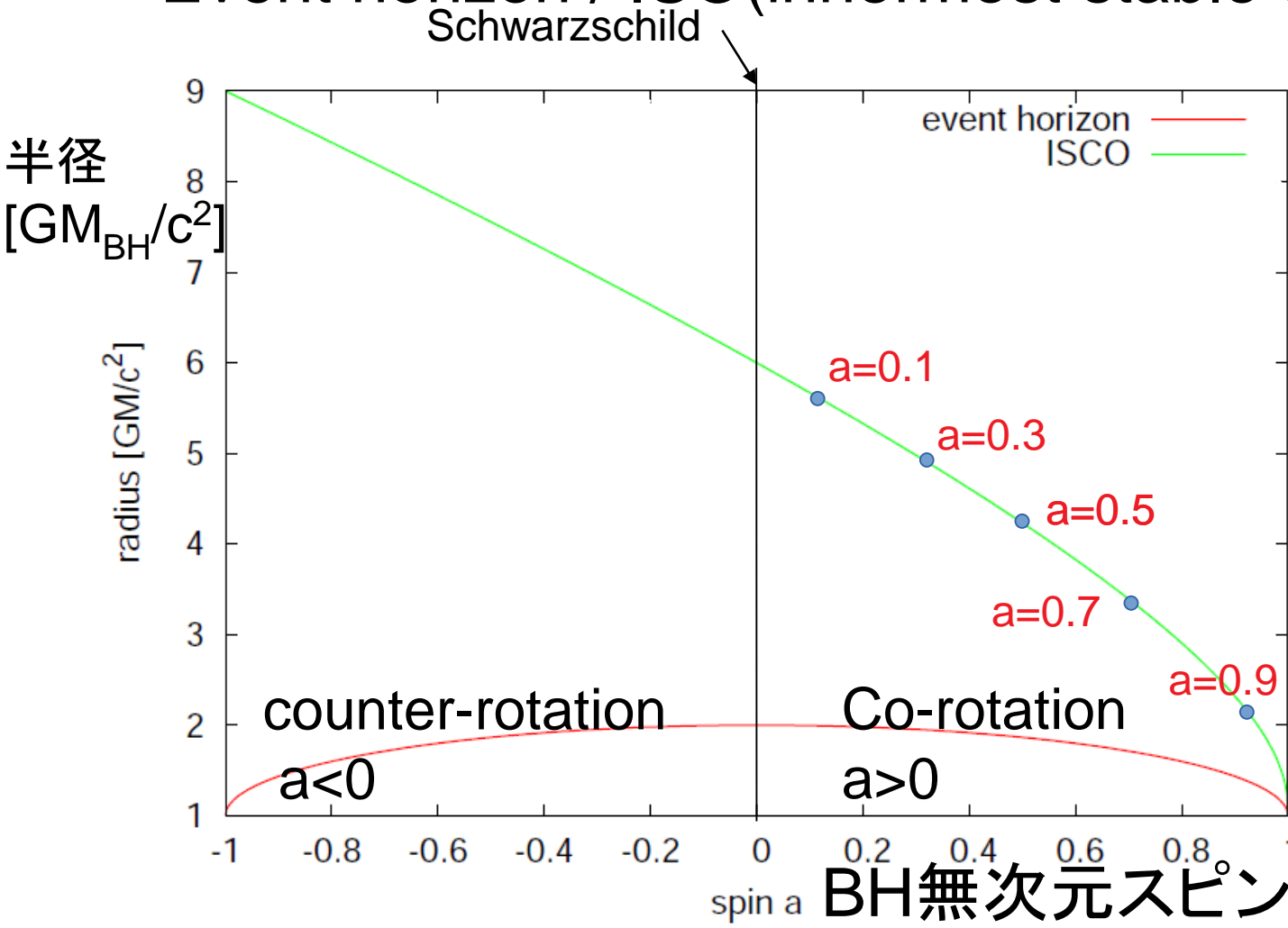
# 磁気浮力



from Machida  
+2014

Parker Instability (1966) enhances generation of poloidal B.

# Event horizon / ISCO(innermost stable circular orbit)



Both  $r_H$  and  $r_{ISCO}$  approaches  $r=1$  as  $a \rightarrow 1$  (maximum spin)

• Since B-field amplification occurs in the disk ( $r > r_{ISCO}$ ), the timescale of B-field amplification may depend on Kerr-spin parameter.

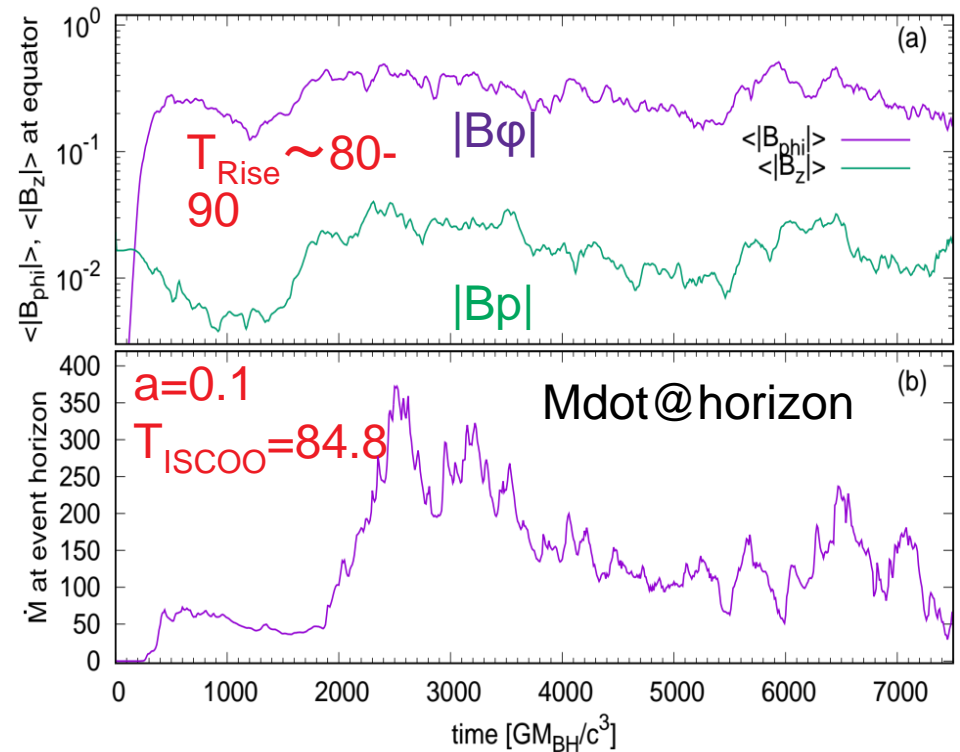
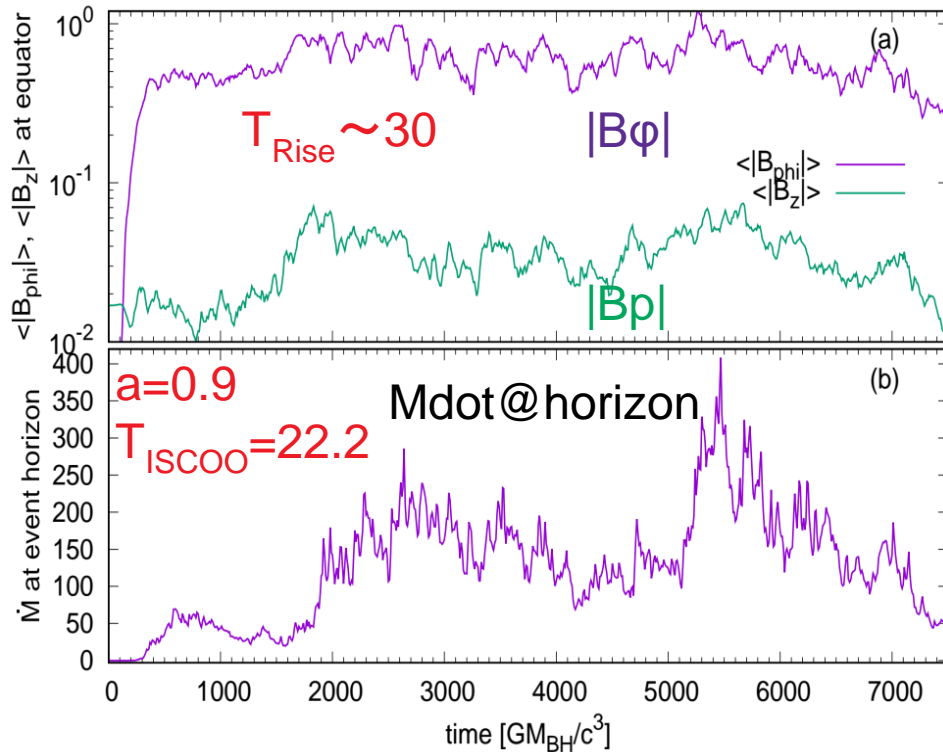
$$r_H = 1 + \sqrt{1 - a^2} \quad (g_{rr} = 0 \text{ @ Boyer-Lindquist})$$

$$r_{ISCO} = 3 + g(a) \mp \sqrt{[3 - f(a)][3 + f(a) + 2g(a)]}$$

$$f(a) \equiv 1 + (1 - a^2)^{1/3} [(1 + a)^{1/3} + (1 - a)^{1/3}]$$

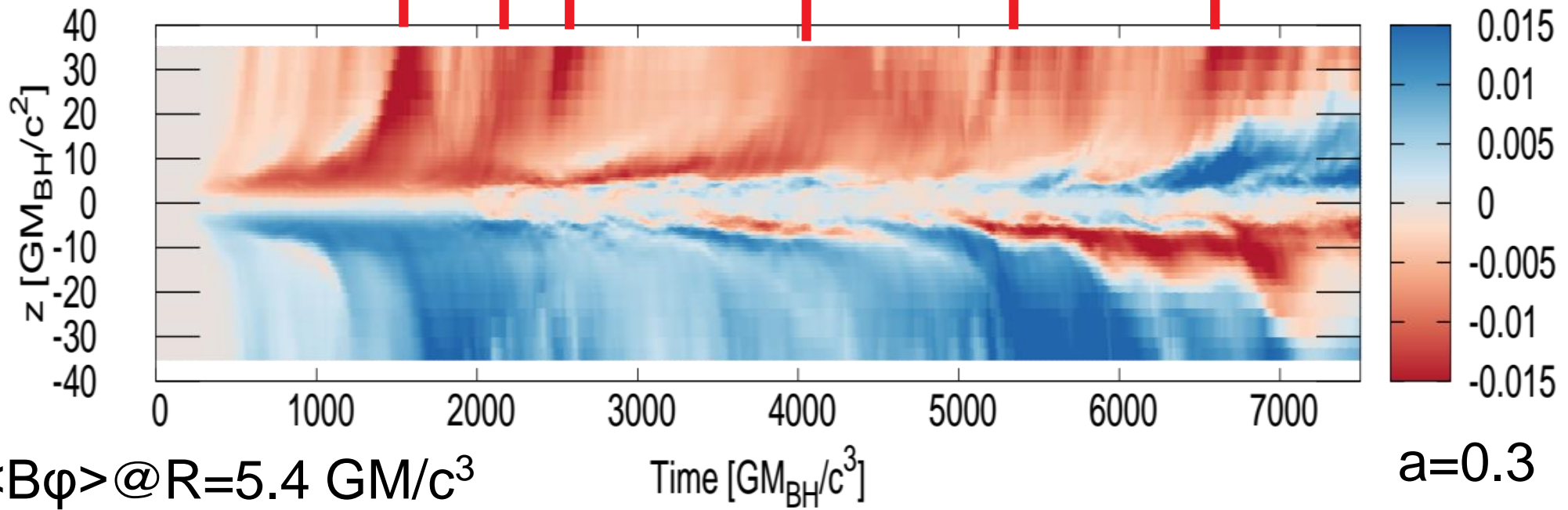
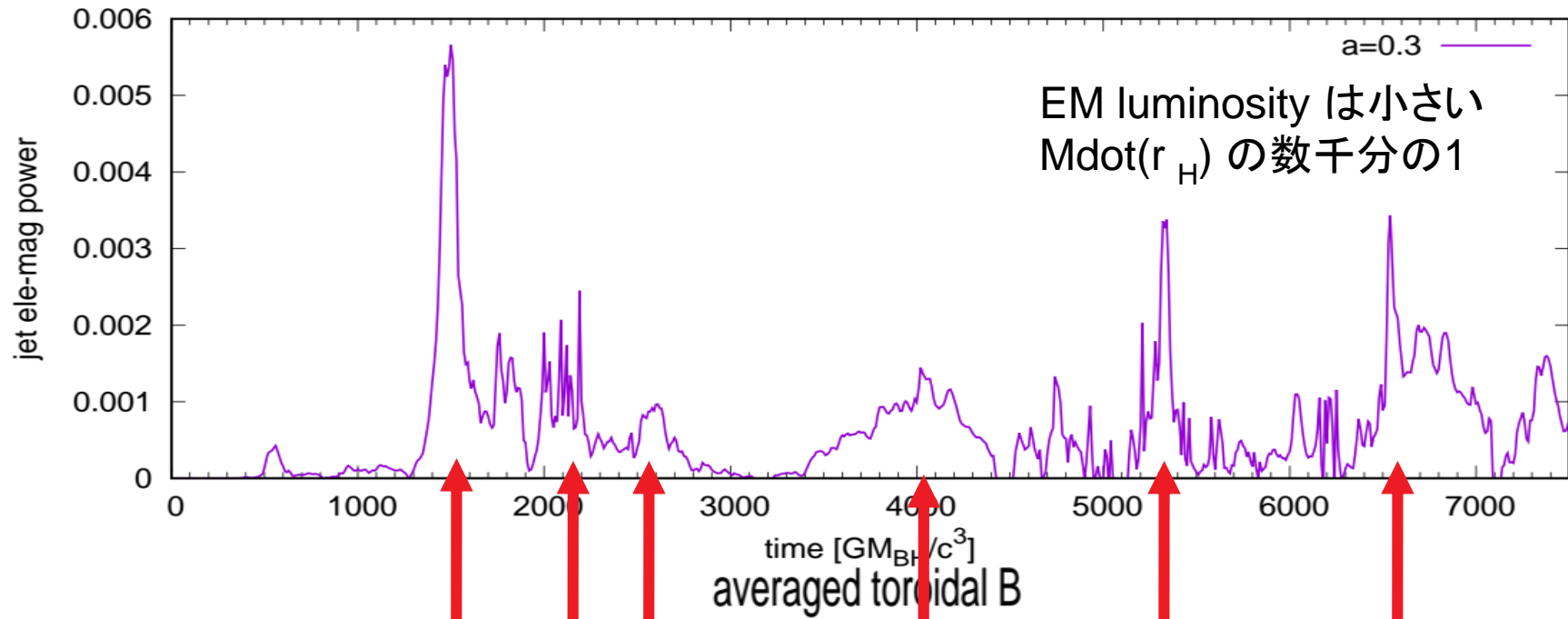
$$g(a) \equiv \sqrt{(3a^2 + f(a)^2)}$$

# スピンパラメータ(a)依存性：磁場増幅の時間スケール



- スピンパラメータ  $a$  が小さくなるにつれ、磁場増幅、質量降着率の時間変動は長くなる
- その時間スケールは ISCO 半径のやや外側でMRIによる磁場増幅の最大成長率のモードの時間スケール程度

# Butterfly diagram & EM jet power

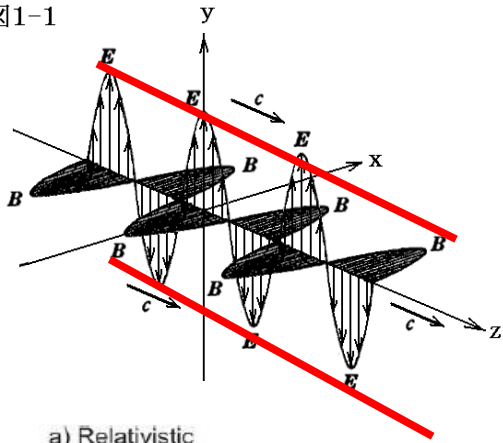




# Wakefield acceleration (Tajima & Dawson PRL 1979)

Acceleration mechanism by interaction between wave and plasma.

☒1-1



Laser plasma interaction  
 $\Rightarrow$  8 shape motion.

$$\mathbf{F} = q \left( \mathbf{E} + \frac{\mathbf{v}}{c} \times \mathbf{B} \right)$$

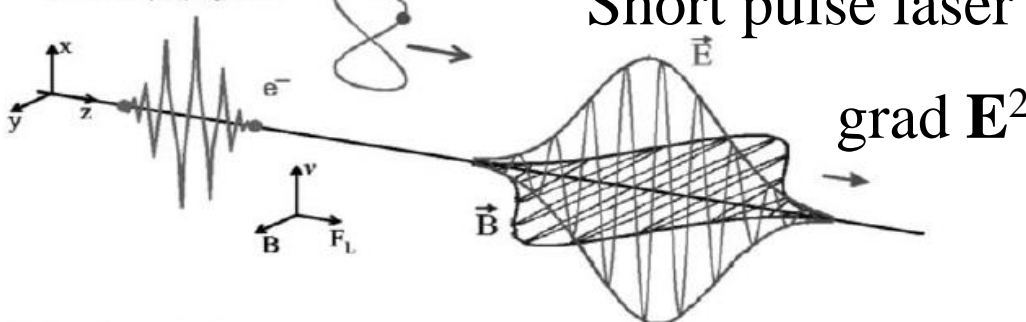
Oscillation by Electric field  $\Rightarrow \mathbf{v}$   
 (oscillation up, down)  
 $\mathbf{v} \times \mathbf{B}$  force  $\Rightarrow$  oscillation forward  
 and backward.

$|\mathbf{v}| \sim c \Rightarrow$  large amplification motion  
 by  $\mathbf{v} \times \mathbf{B}$ . (8 shape motion).

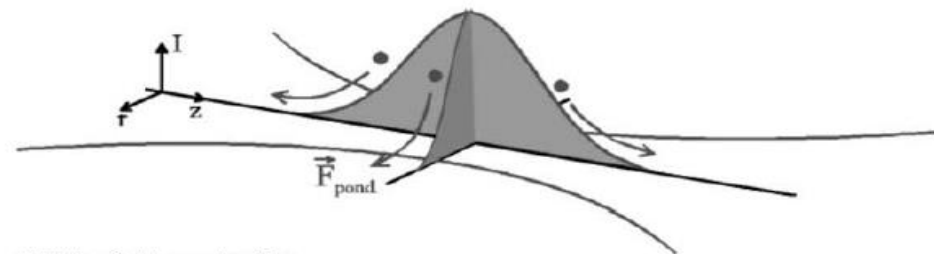
If there is gradient in  $E^2$ , charged particles feel the force towards less  $E^2$  side. = "Ponderomotive force"

Effective acceleration for  
 $I \sim 10^{18} \text{ W/cm}^2$  (relativistic intensity).  
 Experimentally observed.

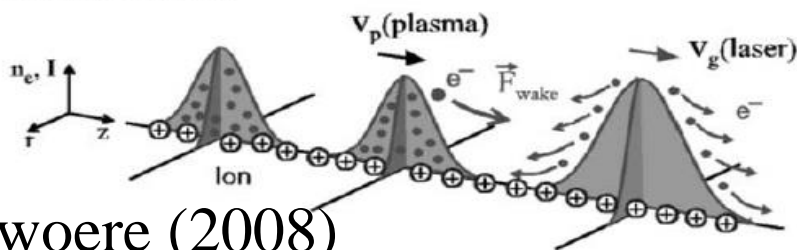
a) Relativistic electron propagation



b) Ponderomotive force



c) Wake field acceleration



Schwore (2008)

Relativistic Alfvén wave can be applied to wakefield acceleration. (Takahashi+2000, Chen+2002, Lyubarusky 2006, Hoshino 2008)

# Ponderomotive 力による粒子加速

- strength parameter  $a_0$  at maximum peak in Alfvén flare highly exceeds unity as estimated in Ebisuzaki & Tajima (2014);

$$a_0 = \frac{eE}{m_e \omega_{AC}} = 8.8 \times 10^{10} \left( \frac{M}{10^8 M_\odot} \right)^{1/2} \left( \frac{\dot{M}_{av} c^2}{0.1 L_{Ed}} \right)^{1/2}$$

- ジェットの密度が下がることにより Alfvén wave  $\Rightarrow$  EM wave  
Ponderomotive 力によって荷電粒子が加速される

relativistic Alfvén wave

electrons

1:1

protons

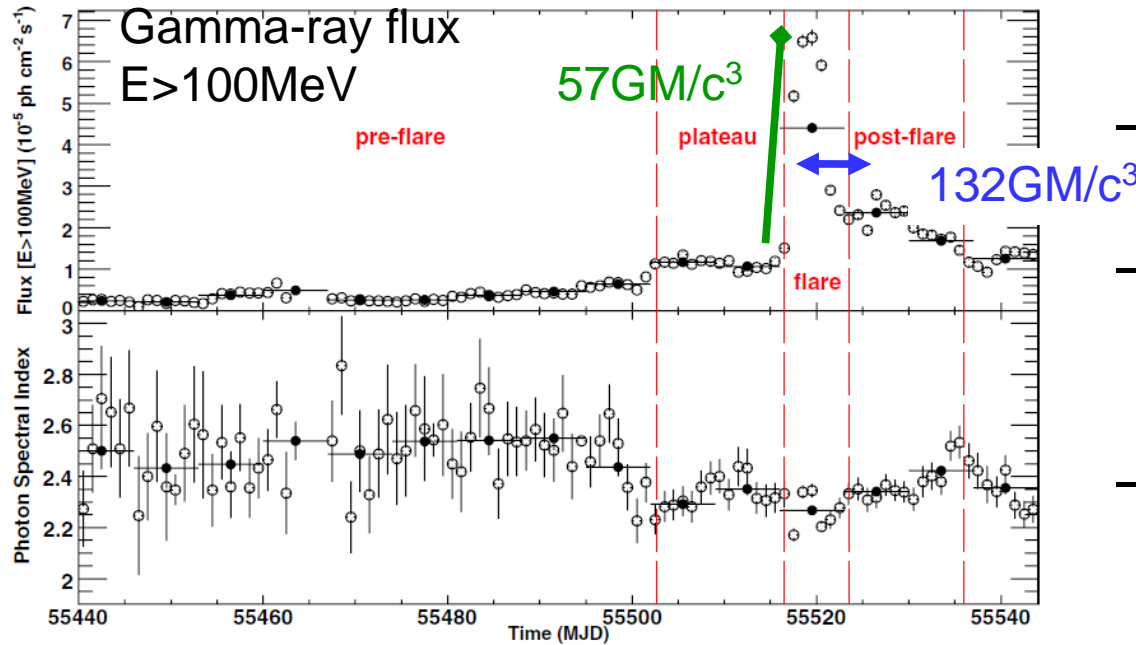
gamma-rays

cosmic rays

– blazars

Ebisuzaki & Tajima 2014

# フェルガンマ線観測衛星によるガンマ線フレア



Fermi observation Abdo + ApJ 2010

	our results	3C454.3	AO0235+164
rising timescale of flares ( $\bar{\tau}_1$ )	30	$57^a$	$325^b$
repeat cycle of flares ( $\bar{\tau}_2$ )	100	$132^a$	$433^b$

3C454.3 ( $M_{\text{BH}} \sim 5 \times 10^8 M_{\text{sun}}$  Bonnoli et al. 2011)

- 相対論的アルフヴェン波の放射 ( $a_0 \gg 1$ )
- 電磁波モードへの変換
- べき的分布をする  
加速された電子 + 磁場
- シンクロトロン放射、  
逆コンプトン放射(ガンマ線)

# まとめ

## 3D GRMHD simulations of rotating BH+accretion disk

- MRI による磁場増幅と磁気散逸に伴う時間変動
  - カースピンパラメータ  $a$  が大きくなると  
時間変動小
- アルフヴェンパルスの放射
  - 赤道面付近での磁場の増幅期から散逸期
  - 円盤鉛直方向
  - 一部はジェットに伝わり、ポインティング成分の  
時間変動の起源に
  - 荷電粒子の加速(proton:UHECR, electron blazars)

今後 極軸付近を含めた高解像度計算  
円盤から放射されるアルフヴェン波の伝播